Probing the valence band structure of Cu_2O using high-energy angle-resolved photoelectron spectroscopy

Anneli Önsten,[1,*] Martin Månsson,[1] Thomas Claesson,[1] Takayuki Muro,[2] Tomohiro Matsushita,[2] Tetsuya Nakamura,[2] Toyohiko Kinoshita,[2] Ulf O. Karlsson,[1] and Oscar Tjernberg[1]

[1]*Materials Physics, Royal Institute of Technology KTH, S-164 40 Kista, Sweden*

[2]*Japan Synchrotron Radiation Research Institute (JASRI), SPring-8, Sayo, Hyogo 679-5198, Japan*

(Received 14 June 2007; published 26 September 2007)

We present angle-resolved photoemission data along the M-Γ-M direction from a $Cu_2O(111)$ single crystal, collected at high photon energies ($h\nu$=619 and 891 eV) and T=100 K. Because of the high photon energies and effective background subtraction, our data give a clear picture of the bulk band structure. The results confirm the existence of a hybridized Cu 3d–Cu 4s state located between the two main Cu 3d and O 2p band regions. Several theoretical studies have predicted the existence of this band, but until now it has not been detected in any photoemission measurements. The experimentally derived band structure is compared to local density approximation calculations with and without the Hubbard potential U. The clear band dispersion in our experimental data has enabled us to extract a refined Hubbard U value, which makes it possible to achieve a better agreement between theoretically calculated bands and experimental data.

DOI: 10.1103/PhysRevB.76.115127 PACS number(s): 79.60.−i, 71.20.−b

I. INTRODUCTION

Cuprous oxide, Cu_2O, is a p-type semiconductor with a direct band gap of 2.17 eV and potential applications in, e.g., solar energy conversion[1] and catalysis.[2] Since the 1950s, it has gained considerable attention because of its rich excitonic spectra and long-lived excitons.[3–5] Later on, the bonding and electronic structure in cuprous oxide and cupric oxide, CuO, have been thoroughly studied in order to achieve a better understanding of the high-temperature superconductivity observed in more complex cuprate materials.

Cu_2O has a simple cubic structure where oxygen atoms form a bcc lattice and every oxygen atom is surrounded by a tetrahedron of copper atoms. Each copper atom thus binds to two oxygen atoms in an unusual linear fashion, a type of bonding that is also present in the CuO_2 planes in high-T_c superconductors. Alternatively, the structure can be described as two independent cristobalitelike sublattices which are not connected with any Cu-O bonds.

There is a controversy in the literature about the charge distribution and bonding in Cu_2O.[6–14] As a first approximation, Cu_2O is often considered to have a closed shell ($3d^{10}$) configuration, giving ionic bonding with spherically symmetric Cu^+ and O^{2-} ions. However, there is quite a strong consensus[6–9,12–15] that such bonding cannot alone explain the stability of this material. Two common arguments for this are that the two interpenetrating networks would repel each other due to the short Cu-Cu and O-O distances and that the linear O-Cu-O bond would be unstable in case of a complete ionization.[14] In 1958, the stability of such linear bonds was explained with 3d-4sp mixing that would compensate for the low coordination number of copper atoms.[16] Furthermore, cluster calculations have shown that short Cu-Cu separations in Cu(I) complexes could be explained with d^{10}-d^{10} interactions between copper atoms, also made possible by Cu 3d–Cu 4sp hybridization.[17]

Zuo *et al.*[6] presented Cu_2O data from x-ray and electron diffraction measurements treated with multipole-model fitting. The results showed a nonspherical charge distribution around the copper atoms and an unexpectedly high amount of charge at the empty tetrahedral Cu_4 site. The authors suggested this to be due to the hybridization of Cu 3d and Cu 4sp orbitals and the covalent bonding between Cu atoms. In contradiction to these results, Lippmann and Schneider[10,11] could not deduce any interstitial Cu_4 charge density maximum from their synchrotron x-ray diffraction data. They also showed that the charge transfer from Cu to O was only 0.4–0.6 electrons compared to one electron, as predicted in the study of Zuo *et al.* This was confirmed by theoretical studies,[7,9,12] where the calculations gave $Cu^{+(0.5–0.84)}$ ions and no local charge density maximum at the tetrahedral site.

Although the stabilization of the Cu_2O structure is a controversial subject, several studies[6,7,11,14,15,18] agree that the charge density around copper atoms is not fully spherical. Many studies also predict an intraatomic Cu 3d–Cu 4sp hybridization[12,14–17,19,20] that could explain the aspherical symmetry. However, the extent of this hybridization is still not clear. A recent study[12] suggests that most of the charge in the Cu 4s orbital is due to an incomplete ionization and that only a minor part comes from the Cu 3d orbital. An analysis of the electron localization function made by the same group showed weak metallic interactions between copper atoms by the sharing of Cu 4sp electrons.

Since the 1980s, several band structure calculations have been performed on Cu_2O, among them Hartree-Fock studies,[13,21] cluster calculations,[18] empirical linear combination of atomic orbital studies,[22] first-principles orthogonalized linear combination of atomic orbitals studies,[23] linearized augmented plane-wave calculations within the muffin-tin approximation,[15] local density approximation (LDA) calculations,[12,20,24] pseudopotential-like self-interaction corrected LDA,[12] and self-consistent Green's function calculations with screened Coulomb interaction (scGW).[20,24] The electronic structure of Cu_2O has also been investigated experimentally in a number of photoemission studies,[19,20,24–27]

but to our knowledge, only one of them is angle resolved,[24] measured along the Γ-*R* direction.

In the current study, a clear image of the band structure is obtained from high-energy angle-resolved photoelectron spectroscopy (ARPES) data. The high photon energies used not only increase the bulk sensitivity significantly but also make it possible to directly measure the dispersion along a particular line in reciprocal space (here, *M*-Γ-*M*) in a single measurement. These advantages, together with the specific background subtraction used here, have enabled an experimental proof of the hybridized band that has been predicted to be located between the main Cu 3*d* and O 2*p* band regions. To enable an identification and discussion of visible bands, two types of band structure calculations have been performed. Besides conventional LDA calculations, LDA including the Hubbard *U* potential (LDA+*U*) has also been performed and compared to the experimental data.

II. EXPERIMENTAL DETAILS

In this paper, we present ARPES data from a $Cu_2O(111)$ single crystal, collected at $T=100$ K and at high photon energies ($h\nu=619$ and 891 eV). The azimuthal orientation of the sample was chosen to enable measurements of the dispersion along the *M*-Γ-*M* direction in reciprocal space. The circularly polarized synchrotron light had a 45° angle of incidence relative to the sample surface normal. Data were acquired using a Gammadata Scienta SES-200 electron analyzer at the BL25SU beamline[28] of the SPring-8 synchrotron radiation facility. At photon energies of 619 and 891 eV, the monochromator gives energy resolutions of 120 and 180 meV, respectively. The angular resolutions parallel and perpendicular to the analyzer slit are ±0.1° and ±0.15°, respectively. This gives a momentum resolution of $\sim 0.022/0.033$ Å^{-1} for $h\nu=619$ eV and $\sim 0.027/0.040$ Å^{-1} for $h\nu=891$ eV. In the direction perpendicular to the surface plane, the instrumental *k* resolution is not limiting since the escape depth is on the order of 13 Å, which, in turn, implies a *k* uncertainty of approximately 0.08 Å^{-1}. The base pressure was kept below 2×10^{-10} mbar during the entire acquisition period.

The $Cu_2O(111)$ crystal (<1% calcium content) was acquired from the Surface Preparation Laboratory.[29] It was cleaned through gentle Ar^+ sputtering and subsequent annealing at $T=730$ °C (Ref. 30) until a sharp (1×1) low-energy electron diffraction (LEED) pattern was obtained, as shown in Fig. 1. Acquired O 1*s* and Cu 2*p* core level photoemission spectra were compared with data from an earlier photoemission study[26] on polycrystalline Cu_2O and CuO. The results are consistent with a pure Cu_2O sample.

III. EXPERIMENTAL RESULTS

Figure 2 displays the experimental band dispersion (no background subtraction) along the *M*-Γ-*M* direction in reciprocal space, as obtained with ARPES. To the best of our knowledge, no other ARPES study on Cu_2O along this particular direction has been previously published. The photon energies of 619 and 891 eV were chosen in order to reach

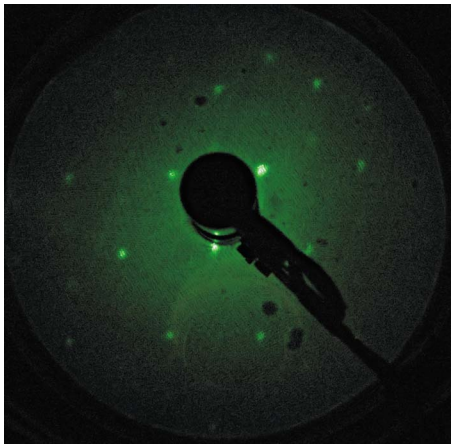

FIG. 1. (Color online) LEED pattern from the clean $Cu_2O(111)$ surface.

two different instances of the Γ point. Energy distribution curves (EDCs) measured at the Γ point are plotted in Fig. 3. Both the angle-resolved photoemission data (Fig. 2) and the EDCs (Fig. 3) are very similar for the two different photon energies, confirming that we, in both measurements, cross the Brillouin zone (BZ) through the Γ point.

One advantage with using high photon energies is that the entire *M*-Γ-*M* line across the BZ can be covered in a single measurement. This is because the angular acceptance of the analyzer ($\theta_{em}=\pm6°$) corresponds to a range of $|k_{\|}|$ on the order of the *M*-Γ-*M* distance in Cu_2O at these energies. Data from emission angles $-4.9°\ldots4.1°$ have been used to plot the band structure in Fig. 2. This range of angles covers 100% and 115% of the *M*-Γ-*M* line for the photon energies of 619 and 891 eV, respectively. Furthermore, at these high

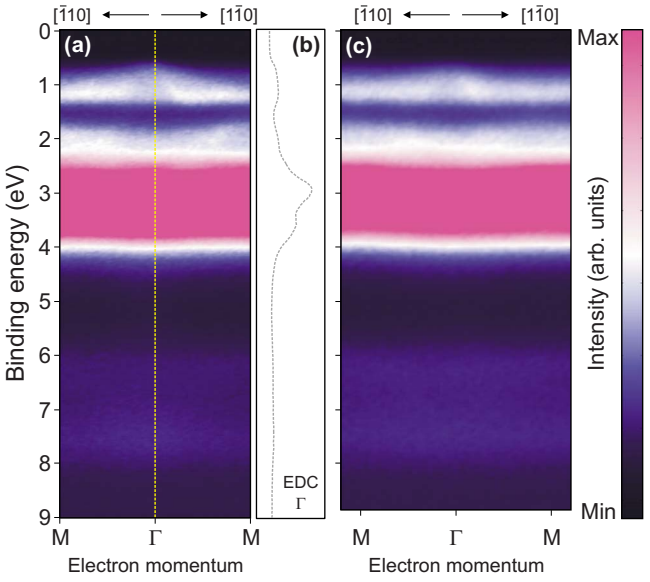

FIG. 2. (Color online) Angle-resolved photoemission data (*M*-Γ-*M*) from Cu_2O (no background subtraction) acquired at $T=100$ K and (a) $h\nu=619$ eV and (c) $h\nu=891$ eV. (b) Energy distribution curve measured with $h\nu=619$ eV at the Γ point.

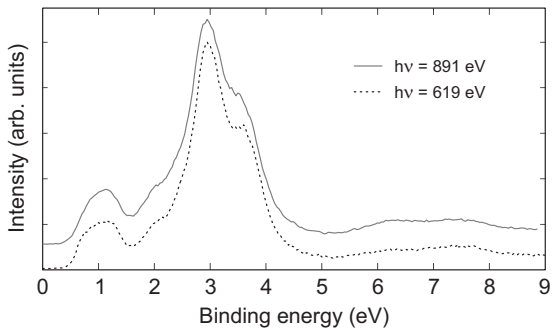

FIG. 3. Energy distribution curves (EDCs) at the Γ point for $h\nu$=619 eV (dashed line) and $h\nu$=891 eV (solid line).

energies, the $k_{\|}$ vector is approximately proportional to the emission angle. Normally, ARPES measurements are performed at lower photon energies (20–100 eV), where it is necessary to perform several measurements at different photon energies and/or emission angles to reach across the BZ. In addition, at lower photon energies, one has to resort to the assumption of a free-electron-like final state to extract the k-resolved band structure from the ARPES data. This is not necessary in the present high-energy study. Another advantage with high photon energies is the longer mean free path of photoemitted electrons, giving increased bulk sensitivity.

Due to indirect transitions in the photoemission process[31] and a nonperfect sample surface, the untreated experimental data (Fig. 2) are dominated by k-independent background intensity. In order to extract and clearly display the k-dependent intensity superimposed on this background, it is necessary to perform a background subtraction. In Fig. 4, this has been achieved by a two-step process. First, the intensity in each EDC has been normalized to unity in order to correct for variations in detection efficiency along the angular direction. (This normalization condition is reasonable in the present case since Cu_2O has no bands crossing the Fermi level.) Second, a constant background has been subtracted from each momentum distribution curve (MDC). The value of the subtracted background for each MDC is chosen as the mean value of the MDC, rather than the minimum value, in order to minimize the statistical noise. As seen from a comparison between Figs. 2 and 4, this background subtraction is very efficient in extracting the k-dependent intensity. On the other hand, one has to keep in mind that the information about absolute intensities is lost. The absence of the strongest feature in the spectra [D1 in Fig. 4(b)] around the Γ point is perhaps the clearest such effect. Finally, since the MDCs are symmetric around the Γ point, the statistics in the data has also been improved by symmetrizing the data around the Γ point. Overall, this treatment of the data gives a clearer image of the band structure, which is obvious when comparing Fig. 4 with Fig. 2.

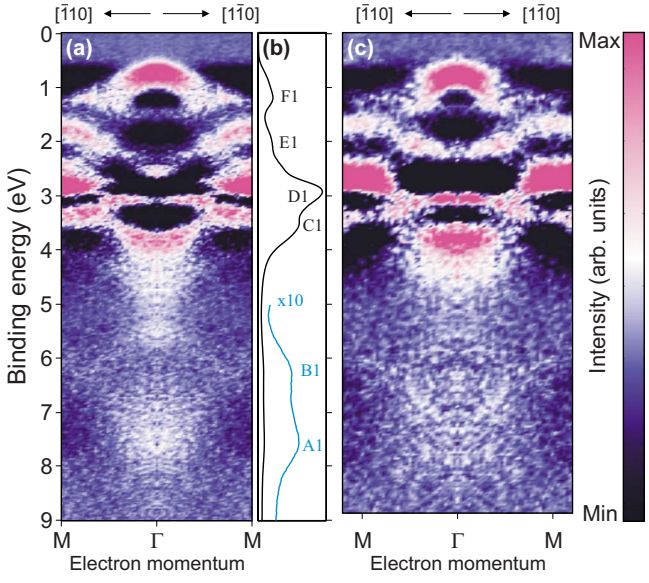

FIG. 4. (Color online) Background-subtracted and symmetrized angle-resolved photoemission data (M-Γ-M) from Cu_2O acquired at T=100 K and (a) $h\nu$=619 eV and (c) $h\nu$=891 eV. The intensity color scale is the same in both panels. (b) An angle-integrated spectrum measured at $h\nu$=619 eV.

TABLE I. Binding energies for band structure features in Cu_2O from experimental angle-integrated spectra and broadened theoretical density of states.

Features	Fig. 4(b) (eV)	Ref. 25 (eV)	LDA, Fig. 6(c) (eV)	LDA+U, Fig. 6(d) (eV)
A1	7.5	7.25	7.75	7.45
B1	6.3	6.04	6.2	5.93
C1	3.52	3.37	2.9	3.58
D1	2.93	2.95	2.4	2.93
E1	2.1	2.00	1.7	2.11
F1	1.17	1.01	1.2	1.13

The Cu_2O valence band structure has previously been shown to consist of two main regions of bands, where one region ($E_{bin} \approx 1-4$ eV) is dominated by Cu 3d states, while the other region ($E_{bin} \approx 6-7$ eV) has a more pronounced O 2p character.[20,26] Six different band structure features, referred to as A1, B1, C1, D1, E1, and F1 [see Fig. 4(b)], have been identified in an earlier resonant photoemission study,[25] where each feature is associated with a band or a group of bands. A1 and B1 were shown to mainly be oxygen features with some copper character for A1, while C1–F1 predominantly had copper character with an oxygen part in F1. These features are all present in the angle-integrated spectrum in Fig. 4(b); their binding energies are listed in Table I and orbital characters in Table II. Most theoretical calculations have also predicted a dispersive mixed Cu 3d-4s state, here labeled by its symmetry character Γ_1, situated between the main Cu 3d and O 2p band regions. However, this state is not visible in any of the photoemission spectra in the literature. The Γ_1 band can be distinguished in the binding energy region of 4–5 eV of our ARPES data presented in Fig. 4(a) and is clearly seen in Fig. 7. In the latter figure, the data in the binding energy range of 4–9 eV have been replotted with a more appropriate numerical interval for the color intensities. Table II lists the results from an analysis of the atomic orbital character of the different states made by

TABLE II. Orbital characters at the Γ point for band structure features in Cu_2O and their corresponding binding energies (E_{bin}) as calculated by Bruneval within the LDA and listed in Table 12.4 in Ref. 20.

E_{bin}[a] (eV)	Cu 3*d* (%)	Cu 4*s* (%)	O 2*p* (%)
7.89	30	8	61
5.44	0	0	98
5.47	36	60	0
2.12–3.58	⩾98	⩽2	0
0.60	68	12	20

[a]The binding energy has been adjusted by +0.60 eV as compared to Ref. 20.

Bruneval.[20] The Γ_1 band was there predicted to have a character that is 60% Cu 4*s* and 36% Cu 3*d* at the Γ point. An additional state [L_1, Fig. 6(a)] visible in both our data and in the data of Bruneval *et al.*[24] is situated around 1.5 eV at the Γ point. This nondispersive state does not exist in in any of the theoretical studies found in the literature.[12,13,20,22,23]

IV. BAND STRUCTURE CALCULATIONS

In order to compare the band structure, as measured by ARPES, with predictions from theory, we have performed band structure calculations (Fig. 5) in the LDA. In a recent study, Laskowski *et al.*[14] performed LDA+*U* calculations on Cu_2O using different forms of the LDA+*U* correction. The authors found that an improved description of the electronic structure was attained using the self-interaction corrected form of the potential introduced by Anisimov *et al.*[32] To test this theory, we have also performed similar LDA+*U* band structure calculations. Through comparisons of LDA+*U* density of states (DOS) [Fig. 5(b)] with the angle-integrated spectrum [Fig. 4(b)] and calculated bands [Fig. 5(a)] with ARPES data [Fig. 4(a)], we have found that the values $U=0.45$ Ry and $J=0.07$ Ry for Cu 3*d* orbitals result in a generally good agreement (Fig. 6). For reference, we have also performed LDA+*U* calculations using the literature values $U=0.59$ Ry and $J=0.07$ Ry.[14] The result is presented in Fig. 6(e). All calculations were performed using the WIEN2k software package[33] and a cubic Cu_2O lattice with $a=4.27$ Å.

The resulting band structure from our calculations along the Γ-*M* direction is displayed in Fig. 5(a) and that on top of the corresponding ARPES valence band data in Figs. 6(a), 6(b), and 7(b). Our LDA results agree well with earlier LDA calculations.[20] The unbroadened DOS from LDA/LDA+*U* calculations is shown in Fig. 5(b). To simulate the effect of instrumental resolution, we have applied a Gaussian broadening of 120 meV on the LDA/LDA+*U* DOS. The result is shown in Figs. 6(c)–6(e) next to an angle-integrated photoemission spectrum in Fig. 6(f). The LDA and LDA+*U* calculations have all been displaced by ~0.6 eV in order to align the valence band maximum to the ARPES data. Some of the peak positions of the broadened DOS are listed in Table I. When comparing the broadened DOS to the experimental angle-integrated spectrum, it is important to bear in mind that the photoionization cross sections for O 2*p* and Cu 4*s* are much smaller than that for Cu 3*d*. Cross sections for different energies and orbitals are listed in Table III.

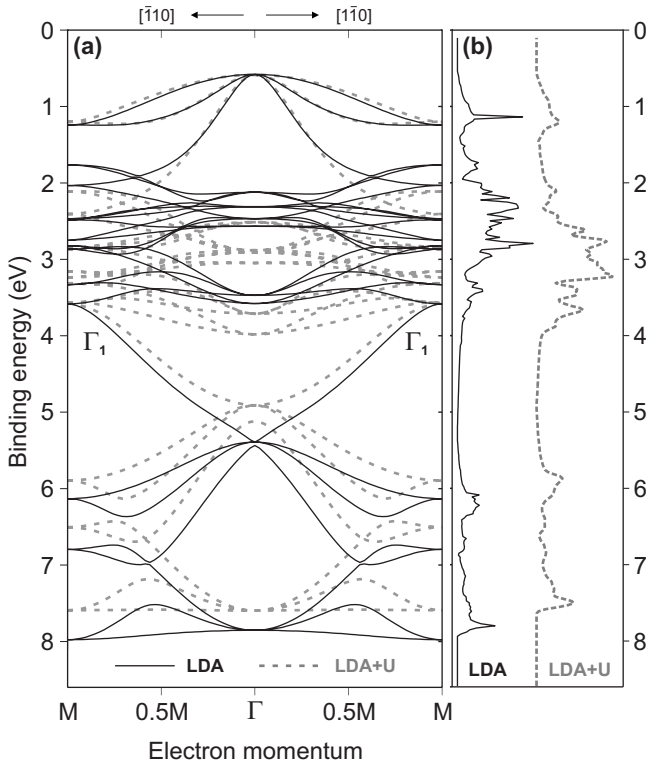

FIG. 5. (a) LDA (solid lines) and LDA+*U* (dashed lines [$U=0.45$ Ry and $J=0.07$ Ry]) band structure calculations on Cu_2O along the *M*-Γ-*M* line. (b) Unbroadened density of states from LDA (solid line) and LDA+*U* (dashed line).

V. DISCUSSION

The only other ARPES study on Cu_2O until now is a recently published work from Bruneval[20] and Bruneval *et al.*[24] Contrary to our study, their data were acquired along the Γ-*R* direction, at room temperature and at low photon energies (20–46 eV). One of the aims of their investigation was to find the hybridized Cu 3*d*–Cu 4*s* band (Γ_1), whose existence had not been proven experimentally. By performing ARPES measurements, they hoped to make this band visible. They argued that since earlier photoemission studies only presented angle-integrated spectra, the Γ_1 band might have been averaged out because of its high dispersion. However, their study did not prove its existence, which they explained by the low cross section of the Cu 4*s* orbital, the large amount of secondary electrons, and the high dispersion of the band.

Bruneval *et al.* presented their two-dimensional ARPES data in the form of the second derivative of the photoelectron intensity from which a Shirley background[35] was subtracted. In our study, the intensity itself is plotted, which gives a more direct description of the data. Our experimental valence band data have many similarities with those obtained by

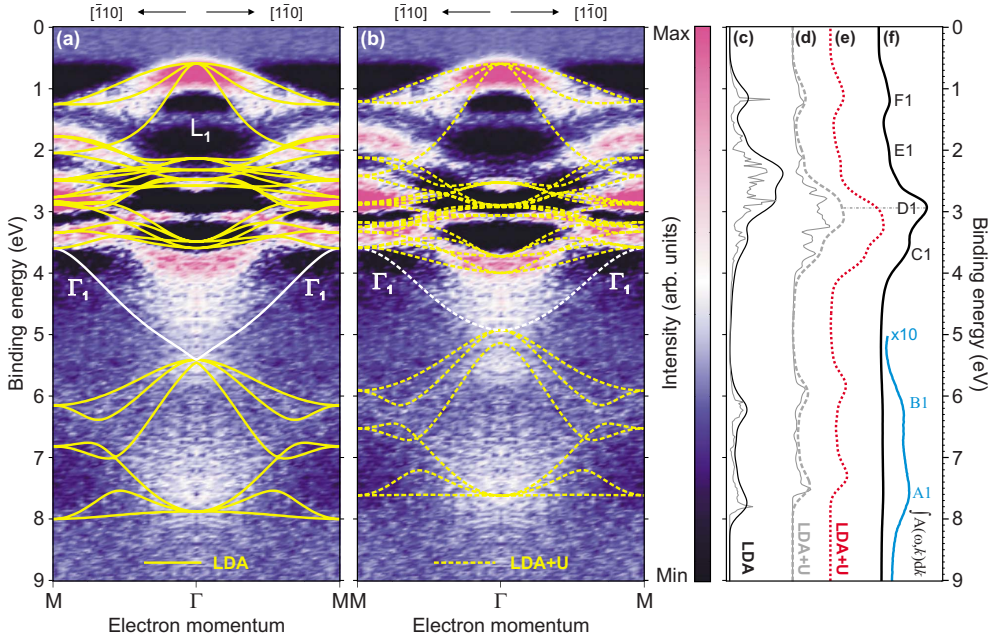

FIG. 6. (Color online) (a) LDA (solid lines) band structure calculations compared to angle-resolved photoemission data (M-Γ-M) measured at $h\nu$ =619 eV. (b) LDA+U (dashed lines) band structure calculations compared to angle-resolved photoemission data (M-Γ-M) measured at $h\nu$=619 eV. (c) LDA DOS (thin line) and broadened LDA DOS (thick line). (d) LDA+U DOS (thin line) and broadened LDA+U DOS (thick dashed line) using the refined U value 0.45 Ry and J=0.07 Ry. (e) Broadened LDA+U DOS (red dotted line) using literature values U=0.59 Ry and J=0.07 Ry. (f) Angle-integrated spectrum $[\int A(\omega,k)dk]$ measured at $h\nu$ =619 eV.

Bruneval *et al.*[24] but give more clearly distinguished bands and show several features that are weak or not visible in their study. The most obvious such features are the Cu 3d bands in the binding energy range of 1.7–2.6 eV, represented by E1 in Fig. 6(f), and the Γ_1 band at energies of 4.0–4.6 eV, also shown in Fig. 7. One possible reason why these bands are clearly visible in our study and not in Ref. 24 might be the difference in cross section ratios (see Table III). At the higher photon energies used in our study, the O 2p/Cu 3d cross section ratio is much lower and the Cu 4s/Cu 3d cross section ratio is approximately two times higher. Another possibility is that these bands are easier to distinguish in the Γ-M direction as compared to the Γ-R direction. In addition, these two experimental studies also differ in terms of bulk sensitivity (photon energies) and data treatment.

Due to its nearly closed Cu 3d shell, Cu_2O is considered as the cuprate material with the simplest electronic structure, which is why it is often used for studying the O-Cu-O bond. In spite of this, the agreement between band structure calculations and photoemission experiments found in the literature has not been completely satisfactory. Laskowski *et al.*[14] concluded that LDA and generalized gradient approximation calculations tend to overestimate the Cu 3d–Cu 4s hybridization. On the other hand, a better description of the charge density and electric field gradients in Cu_2O was obtained using the LDA+U method.[14] Encouraged by this fact, we have performed LDA and LDA+U band structure calculations, which we compare to our experimental data. It should, however, be noted that LDA calculations are known to give an incomplete description of the electronic band structure in 3d systems such as transition metal oxides.

In Figs. 5 and 6, the energy band structure and DOS from LDA/LDA+U calculations are shown. Clear differences are revealed between the conventional LDA and LDA+U methods. The inclusion of a repulsive potential U shifts the Cu 3d bands and, hence, the features C1 and D1 [Figs. 6(c) and 6(d)] to higher binding energies. The O 2p bands and, hence, the features A1 and B1 [Figs. 6(c) and 6(d)] are, nevertheless, moved to lower binding energies. The LDA+U method also gives a smaller dispersion for the Γ_1 band, as seen in Figs. 6(b) and 7(b). Overall, this method gives a smaller width of the valence band than what is obtained with the

TABLE III. Photoionization cross sections (Mb) of atomic orbitals for different photon energies $h\nu$ from Ref. 34.

$h\nu$ (eV)	Cu 3d (Mb)	Cu 4s (Mb)	Cu 2p (Mb)
21.2	7.6	0.036	10.7
40.8	9.9	0.041	6.8
600	0.15	0.0014	0.0061
800	0.077	0.00089	0.0022
1041	0.036	0.00055	0.00089

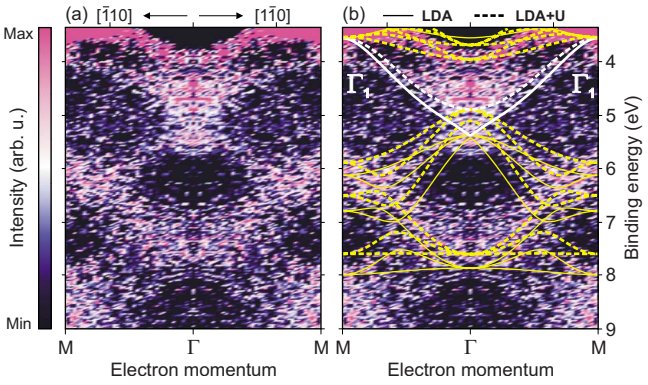

FIG. 7. (Color online) (a) Cu_2O angle-resolved photoemission data ($h\nu$=619 eV) in the binding energy range of ~4–9 eV. (b) Data from (a) compared to LDA (solid lines) and LDA+U (dashed lines) band structure calculations.

LDA calculation. These changes are significant compared to the effects of the scGW calculations performed by Bruneval *et al.*[24] The scGW calculations also give a larger displacement between features D1 and F1, and the dispersion of the hybridized Cu $3d$–Cu $4s$ band is lowered somewhat, but not to the extent obtained with the LDA+U method.

The LDA+U method is described in Refs. 14 and 32 and normally gives a good description of strongly correlated systems with localized electrons. This method gives less Cu $3d$–Cu $4s$ hybridization and an increased occupation of Cu $3d$ orbitals, which results in the observed shift of these orbitals to higher binding energies.[14] Figures 6(a) and 6(b) show the band structure calculations on top of the ARPES data. The LDA and LDA+U calculations have been displaced by ~0.6 eV in order to align the valence band maximum to the ARPES data in Fig. 6. Figures 6(d) and 6(e) display DOS from the LDA+U calculations performed with two different sets of U and J values. The refined U value gives a somewhat lower binding energy for the Cu $3d$ states in C1 and D1 and a slightly higher binding energy of the bands in features A1 and B1 [see Fig. 6(d)] compared to what was obtained with the U and J values used in Ref. 14 [see Fig. 6(e)].

When comparing the experimentally derived valence band structure with band structure calculations, the LDA+U method gives a better fit of the Cu $3d$ states in features C1 and D1 than LDA. As expected, the LDA+U method gives an improved description of the localized Cu $3d$ states. Also, when considering the Γ_1 band (see Fig. 7), it is a better choice. The dispersion of the Γ_1 band in the LDA calculation is much too strong, while it is well reproduced with LDA+U when applying our refined value U=0.45 Ry. The latter method might thus give a more accurate picture of the Cu $3d$–Cu $4s$ hybridization than the conventional LDA method.

There are also bands that are better described by the conventional LDA calculations, e.g., the dispersive band where E_{bin}=1.8 eV at the M point. In the LDA+U calculations, the binding energy of this band is approximately 0.3 eV too high. The difference in binding energy between the O $2p$ states (A1 and B1) and the Cu $3d$ states (C1 and D1) is too large for both LDA and scGW but too small for LDA+U. When considering the binding energies for the oxygen features A1 and B1, the LDA+U calculations thus lead in the right direction, but the step in this direction is slightly too large, even when using our refined value U=0.45 Ry. When the literature U and J values from Ref. 14 were used, this binding energy difference was even smaller and the dispersion of the Γ_1 band was too small, giving a less accurate agreement than for U=0.45 Ry. Additionally, the experimental data in the lower part of Fig. 7 ($E_{bin} \geqslant 8$ eV) display a clear dispersion toward higher binding energy in going from Γ to M. Yet, such dispersion is visible neither in the LDA nor in the LDA+U calculations.

The dispersion of the Γ_1 band and the bands in features E1 and F1, as well as the relative placement of the Cu $3d$–O $2p$ band regions, might be a key to revealing the extent of the Cu $3d$–Cu $4s$ and Cu $3d$–O $2p$ hybridizations in Cu_2O. More knowledge about the mixing of orbitals in Cu_2O might, in its turn, help to explain how the two cristobalitelike sublattices in the cuprite structure stabilize. To obtain a greater understanding in this field, the theoretical methods have to be further developed to better fit experimental data.

While most photoemission experiments are highly surface sensitive, band structure calculations concern, in general, the bulk band structure. This might partly explain the minor discrepancies between theoretical and experimental investigations of the band structure of Cu_2O. In the present study, the impact of this issue is reduced through increased bulk sensitivity stemming from the use of high photon energies. Nevertheless, the nondispersive state (L_1) around 1.5 eV cannot be associated with any bulk bands, neither in our band structure calculations nor in any of the theoretical studies found in the literature.[12,13,20,22,23] The origin of this state is not clear, but given its lack of dispersion, one could speculate that it is a localized state, e.g., a surface-, impurity-, or defect-derived state. Since the same feature is present in another ARPES study[24] performed under different conditions and with a different data treatment, one cannot ignore the presence of this state.

VI. CONCLUSIONS

We present ARPES data from Cu_2O in the Γ-M direction. The high photon energies used ($h\nu$=619 and 891 eV) increase the bulk sensitivity and make final-state approximations unnecessary, thus giving a very clear picture of the valence band dispersion. Owing to the effective background subtraction used in this study, we are able to distinguish a hybridized Cu $3d$–Cu $4s$ state between the main Cu $3d$ and O $2p$ band regions. The dispersion of this band is not well described by LDA nor by scGW calculations but is closer to the predictions of the LDA+U method. Furthermore, by treating the Hubbard U potential as an adjustable parameter we have been able to achieve a better agreement between calculated results and our experimental data. Through a careful comparison of LDA+U DOS with the angle-integrated spectrum and of calculated bands with ARPES data, we have arrived at a refined Hubbard U value U=0.45 Ry. We conclude that the LDA+U method better describes the localized Cu $3d$ states and the mixing of Cu $3d$–Cu $4s$ orbitals than the conventional LDA method. Although the overall agreement between the experimentally and theoretically determined band dispersions is remarkably good, there are still some minor discrepancies. We hope that the work presented here will stimulate further theoretical advances.

ACKNOWLEDGMENTS

This research has been supported by The Swedish Research Council (VR), the Göran Gustafsson Foundation, the Knut and Alice Wallenberg Foundation, the Swedish Foundation for Strategic Research (SSF), and the Japan Synchrotron Radiation Research Institute (JASRI) through a "Budding Researchers Support Proposal" (Proposal No. 2006B1020).

*onsten@imit.kth.se

[1] V. Georgieva and M. Ristov, Sol. Energy Mater. Sol. Cells **73**, 67 (2002).
[2] M. Hara, T. Kondo, M. Komoda, S. Ikeda, K. Shinohara, A. Tanaka, J. N. Kondo, and K. Domen, Chem. Commun. (Cambridge) **1998**, 357.
[3] M. Hayashi and K. Katsuki, J. Phys. Soc. Jpn. **5**, 380B (1950).
[4] D. P. Trauernicht, J. P. Wolfe, and A. Mysyrowicz, Phys. Rev. B **34**, 2561 (1986).
[5] D. A. Fishman, A. Revcolevschi, and P. H. M. van Loosdrecht, Phys. Status Solidi C **3**, 2469 (2006).
[6] J. M. Zuo, M. Kim, M. O'Keeffe, and J. C. H. Spence, Nature (London) **401**, 49 (1999).
[7] S. G. Wang and W. H. Eugen Schwarz, Angew. Chem., Int. Ed. **39**, 1757 (2000).
[8] J. M. Zuo, M. O'Keeffe, M. Kim, and J. C. H. Spence, Angew. Chem., Int. Ed. **39**, 3791 (2000).
[9] S. G. Wang and W. H. Eugen Schwarz, Angew. Chem., Int. Ed. **39**, 3794 (2000).
[10] T. Lippmann and J. R. Schneider, J. Appl. Crystallogr. **33**, 156 (2000).
[11] T. Lippmann and J. R. Schneider, Acta Crystallogr., Sect. A: Found. Crystallogr. **56**, 575 (2000).
[12] A. Filippetti and V. Fiorentini, Phys. Rev. B **72**, 035128 (2005).
[13] E. Ruiz, S. Alvarez, P. Alemany, and R. A. Evarestov, Phys. Rev. B **56**, 7189 (1997).
[14] R. Laskowski, P. Blaha, and K. Schwarz, Phys. Rev. B **67**, 075102 (2003).
[15] P. Marksteiner, P. Blaha, and K. Schwarz, Z. Phys. B: Condens. Matter **64**, 119 (1986).
[16] L. E. Orgel, J. Chem. Soc. **1958**, 4186.
[17] K. M. Merz, Jr. and R. Hoffmann, Inorg. Chem. **27**, 2120 (1987).
[18] S. Nagel, J. Phys. Chem. Solids **46**, 743 (1985).
[19] J. Ghijsen, L. H. Tjeng, H. Eskes, G. A. Sawatzky, and R. L. Johnson, Phys. Rev. B **42**, 2268 (1990).
[20] F. Bruneval, Ph.D. thesis, Ecole Polytechnique, Palaiseau, France, 2005 (http://theory.lsi.polytechnique.fr/people/bruneval/bruneval_these.pdf).
[21] L. Kleinman and K. Mednick, Phys. Rev. B **21**, 1549 (1980).
[22] J. Robertson, Phys. Rev. B **28**, 3378 (1983).
[23] W. Y. Ching, Y.-N. Xu, and K. W. Wong, Phys. Rev. B **40**, 7684 (1989).
[24] F. Bruneval, N. Vast, L. Reining, M. Izquierdo, F. Sirotti, and N. Barrett, Phys. Rev. Lett. **97**, 267601 (2006).
[25] Z.-X. Shen, R. S. List, D. S. Dessau, F. Parmigiani, A. J. Arko, R. Bartlett, B. O. Wells, I. Lindau, and W. E. Spicer, Phys. Rev. B **42**, 8081 (1990).
[26] J. Ghijsen, L. H. Tjeng, J. van Elp, H. Eskes, J. Westerink, G. A. Sawatzky, and M. T. Czyżyk, Phys. Rev. B **38**, 11322 (1988).
[27] P. Steiner, S. Hüfner, A. Jungmann, V. Kinsinger, and I. Sander, Z. Phys. B: Condens. Matter **74**, 173 (1989).
[28] Y. Saitoh, H. Kimura, Y. Suzuki, T. Nakatani, T. Matsushita, T. Muro, T. Miyahara, M. Fujisawa, K. Soda, S. Ueda, H. Harada, M. Kotsugi, A. Sekiyama, and S. Suga, Rev. Sci. Instrum. **71**, 3254 (2000).
[29] http://www.surface-prep-lab.com
[30] K. H. Schulz and D. F. Cox, Phys. Rev. B **43**, 1610 (1991).
[31] N. J. Shevchik, Phys. Rev. B **16**, 3428 (1977).
[32] V. I. Anisimov, I. V. Solovyev, M. A. Korotin, M. T. Czyżyk, and G. A. Sawatzky, Phys. Rev. B **48**, 16929 (1993).
[33] P. Blaha, K. Schwarz, G. K. H. Madsen, D. Kvasnicka, and J. Luitz, WIEN2k, An Augmented Plane Wave+Local Orbitals Program for Calculating Crystal Properties (Karlheinz Schwarz, Techn. Universität Wien, Austria), 2001.
[34] J. J. Yeh and I. Lindau, At. Data Nucl. Data Tables **32**, 1 (1985).
[35] D. A. Shirley, Phys. Rev. B **5**, 4709 (1972).